Boundary integral equations for an interface linear crack under harmonic loading[☆]

I.I. Mykhailova [*], O.V. Menshykov, M.V. Menshykova, I.A. Guz

Centre for Micro- and Nanomechanics (CEMINACS), School of Engineering, University of Aberdeen, Aberdeen AB24 3UE, Scotland, UK

ARTICLE INFO

ABSTRACT

The present study is devoted to application of boundary integral equations to the problem of a linear crack located on the bimaterial interface under time-harmonic loading. Using the Somigliana dynamic identity the system of boundary integral equations for displacements and tractions at the interface is derived. For the numerical solution the collocation method with piecewise constant approximation on each linear continuous boundary elements is used. The distributions of the displacements are computed for different values of the frequency of the incident tension–compression wave. Results are compared with static ones.

© 2009 Elsevier B.V. All rights reserved.

1. Introduction

Generally, fracture mechanics problems for cracked solids under dynamic loading can be solved using advanced numerical methods, since the analytical solutions are limited to a relatively small number of idealized model problems corresponding to very special geometrical configurations and loading conditions. Previously, a considerable amount of work was devoted to cracked homogeneous materials, particularly to time-harmonic elastodynamic analysis of stationary cracks [1–8]. The case of inter-component cracks received much less attention due to the substantial complications which arise in numerical solution of such problems. Primarily the publications concerning crack fracture in composite materials are focused on static loading. However, understanding the mechanism of dynamic fracture in composite materials becomes more and more important with the increased use of composites in modern engineering, where the components are frequently subjected to dynamic loadings, see for example [9–13].

In the paper [14] the system of boundary integral equations for the general case of an interface crack between two dissimilar elastic materials under dynamic loading was derived. In papers [15–19] the derived integral system was solved numerically by the method of boundary elements for the case of a penny-shaped interface crack under normally incident tension–compression wave. The distributions of displacements and tractions were computed for several typical material properties of half-spaces. It was shown that with decreasing frequency of the loading the dynamic solution tends to the static one, and the obtained numerical results are in a very good agreement with the analytical static solution [20,21].

The present paper is devoted to the plane problem for an interface linear crack of finite length under harmonic external loading. The system of boundary integral equations, derived in [14], is modified in order to increase the stability and the accuracy of the solution, and decrease the solution time. The numerical solution is obtained for the normally incident tension–compression wave. The distributions of the normal and tangential displacements at the bonding interface and the crack surface are investigated for different values of the frequency of the incident wave. The dynamic results are compared with the corresponding static ones [11].
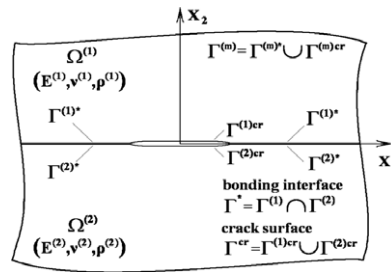
Fig. 1. An interface crack between two half-spaces.

2. Problem statement

Let us consider a linear crack located at the bimaterial interface under external dynamic loading. For this purpose, we investigate an unbounded two-dimensional elastic solid which consists of two dissimilar homogeneous isotropic half-spaces $\Omega^{(1)}$ and $\Omega^{(2)}$. The interface between the half-spaces, Γ^*, acts as the boundary $\Gamma^{(1)}$ for the upper half-space, and the boundary $\Gamma^{(2)}$ for the lower half-space. The boundaries $\Gamma^{(1)}$ and $\Gamma^{(2)}$ differ by the opposite orientation of their outer normal vectors. Henceforth, the superscript (1) refers to the upper half-space and the superscript (2) refers to the lower half-space. We assume that surfaces $\Gamma^{(m)}$ ($m = 1, 2$) consist of the infinite parts $\Gamma^{(m)*}$, which form the bonding interface Γ^*, and the finite parts $\Gamma^{(m)cr}$, which form the crack surface Γ^{cr}, see Fig. 1.

In the absence of body forces, the stress–strain state of both domains is defined by the dynamic equations of the linear elasticity for the displacement vector $\mathbf{u}^{(m)}(\mathbf{x}, t)$ (the Lamé equations)

$$(\lambda^{(m)} + \mu^{(m)})\text{grad div } \mathbf{u}^{(m)}(\mathbf{x}, t) + \mu^{(m)}\Delta\mathbf{u}^{(m)}(\mathbf{x}, t) = \rho^{(m)}\partial_t^2\mathbf{u}^{(m)}(\mathbf{x}, t), \quad \mathbf{x} \in \Omega^{(m)}, t \in T = [0, \infty), \tag{1}$$

where Δ is the Laplace operator, $\lambda^{(m)}$ and $\mu^{(m)}$ are the Lamé elastic constants, $\rho^{(m)}$ is the specific material density.

The following conditions of continuity for displacements and stresses are satisfied at the bonding interface:

$$\mathbf{u}^{(1)}(\mathbf{x}, t) = \mathbf{u}^{(2)}(\mathbf{u}, t), \qquad \mathbf{p}^{(1)}(\mathbf{x}, t) = -\mathbf{p}^{(2)}(\mathbf{x}, t), \quad \mathbf{x} \in \Gamma^* = \Gamma^{(1)} \cap \Gamma^{(2)}, t \in T, \tag{2}$$

where the known traction vectors on the crack surface, caused by the external loading, are given as

$$\mathbf{p}^{(1)}(\mathbf{x}, t) = \mathbf{g}^{(1)}(\mathbf{x}, t), \qquad \mathbf{p}^{(2)}(\mathbf{x}, t) = \mathbf{g}^{(2)}(\mathbf{x}, t), \quad t \in T.$$

It was assumed that there are no initial displacements of the points of the body, in other words the body is strainless at the initial moment.

The Sommerfeld radiation-type condition, which provides a finite elastic energy of an infinite body, is also imposed at infinity on the vector of displacements [5]:

$$\| \mathbf{u}(\mathbf{x}, t) \| \leq C/R, \tag{3}$$

where C is a constant and $R \to \infty$ is the distance from the origin.

3. Integral equations

The components of displacement field in the upper and lower half-spaces $\Omega^{(m)}$ in terms of boundary displacements and tractions can be represented using the Somigliana dynamic identity [1–4,14,15,8]:

$$u_j^{(m)}(\mathbf{x}, t) = \int_T \int_{\Gamma^{(m)}} (p_i^{(m)}(\mathbf{y}, \tau)U_{ij}^{(m)}(\mathbf{x}, \mathbf{y}, t - \tau) - u_i^{(m)}(\mathbf{y}, \tau)W_{ij}^{(m)}(\mathbf{x}, \mathbf{y}, t - \tau))\mathrm{d}\mathbf{y}\mathrm{d}\tau, \quad \mathbf{x} \in \Omega^{(m)}, t \in T, j = \overline{1, 2}, \tag{4}$$

where $\mathbf{x}$ is the point of observation and $\mathbf{y}$ is the point of loading. Here the integral kernel $U_{ij}^{(m)}(\mathbf{x}, \mathbf{y}, t - \tau)$ is the Green fundamental displacement tensor [1–4,8]. The integral kernel $W_{ij}^{(m)}(\mathbf{x}, \mathbf{y}, t - \tau)$ can be obtained from $U_{ij}^{(m)}(\mathbf{x}, \mathbf{y}, t - \tau)$ by applying the following differential operator [2,6]

$$P_{ik}[\bullet, (\mathbf{y})] = \lambda n_i(\mathbf{y})\frac{\partial[\bullet]}{\partial y_k} + \mu\left[\delta_{ik}\frac{\partial[\bullet]}{\partial\mathbf{n}(\mathbf{y})} + n_k(\mathbf{y})\frac{\partial[\bullet]}{\partial y_i}\right] \tag{5}$$

and has the form

$$W_{ij}^{(m)}(\mathbf{x}, \mathbf{y}, t - \tau) = \lambda^{(m)}n_i^{(m)}(\mathbf{y})\frac{\partial}{\partial y_k}U_{kj}^{(m)}(\mathbf{x}, \mathbf{y}, t - \tau) + \mu^{(m)}n_k^{(m)}(\mathbf{y})\left[\frac{\partial}{\partial y_k}U_{ij}^{(m)}(\mathbf{x}, \mathbf{y}, t - \tau) + \frac{\partial}{\partial y_i}U_{kj}^{(m)}(\mathbf{x}, \mathbf{y}, t - \tau)\right].$$

Applying the differential operator (5) to the Somigliana dynamic identity (4) we obtain the components of the traction vector in terms of boundary displacements and tractions for both half-spaces:

$$p_j^{(m)}(\mathbf{x}, t) = \int_T \int_{\Gamma^{(m)}} (p_i^{(m)}(\mathbf{y}, \tau) K_{ij}^{(m)}(\mathbf{x}, \mathbf{y}, t - \tau) - u_i^{(m)}(\mathbf{y}, \tau) F_{ij}^{(m)}(\mathbf{x}, \mathbf{y}, t - \tau)) d\mathbf{y} d\tau, \quad \mathbf{x} \in \Omega^{(m)}, t \in T, j = \overline{1, 2}, \quad (6)$$

where

$$K_{ij}^{(m)}(\mathbf{x}, \mathbf{y}, t - \tau) = \lambda^{(m)} n_i^{(m)}(\mathbf{x}) \frac{\partial}{\partial x_k} U_{kj}^{(m)}(\mathbf{x}, \mathbf{y}, t - \tau) + \mu^{(m)} n_k^{(m)}(\mathbf{x}) \left[\frac{\partial}{\partial x_k} U_{ij}^{(m)}(\mathbf{x}, \mathbf{y}, t - \tau) + \frac{\partial}{\partial x_i} U_{kj}^{(m)}(\mathbf{x}, \mathbf{y}, t - \tau) \right],$$

$$F_{ij}^{(m)}(\mathbf{x}, \mathbf{y}, t - \tau) = \lambda^{(m)} n_i^{(m)}(\mathbf{x}) \frac{\partial}{\partial x_k} W_{kj}^{(m)}(\mathbf{x}, \mathbf{y}, t - \tau) + \mu^{(m)} n_k^{(m)}(\mathbf{x}) \left[\frac{\partial}{\partial x_k} W_{ij}^{(m)}(\mathbf{x}, \mathbf{y}, t - \tau) + \frac{\partial}{\partial x_i} W_{kj}^{(m)}(\mathbf{x}, \mathbf{y}, t - \tau) \right].$$

For the limiting case $\mathbf{x} \to \Gamma^{(m)}$, taking into account the assumed relatively smooth distribution of traction on regular surfaces $\Gamma^{(1)}$ and $\Gamma^{(2)}$, the following representation of the traction vector at the interface can be obtained from Eq. (6):

$$\frac{1}{2} p_j^{(m)}(\mathbf{x}, t) = \int_T \int_{\Gamma^{(m)}} (p_i^{(m)}(\mathbf{y}, \tau) K_{ij}^{(m)}(\mathbf{x}, \mathbf{y}, t - \tau) - u_i^{(m)}(\mathbf{y}, \tau) F_{ij}^{(m)}(\mathbf{x}, \mathbf{y}, t - \tau)) d\mathbf{y} d\tau, \quad \mathbf{x} \in \Gamma^{(m)}, t \in T, j = \overline{1, 2}. \quad (7)$$

Thus, the boundary integral equations on the surfaces $\Gamma^{(1)}$ and $\Gamma^{(2)}$ have the following form:

$$\frac{1}{2} g_j^{(1)}(\mathbf{x}, t) = \int_T \int_{\Gamma^{(1)cr}} (g_i^{(1)}(\mathbf{y}, \tau) K_{ij}^{(1)}(\mathbf{x}, \mathbf{y}, t - \tau) - u_i^{(1)}(\mathbf{y}, \tau) F_{ij}^{(1)}(\mathbf{x}, \mathbf{y}, t - \tau)) d\mathbf{y} d\tau$$
$$+ \int_T \int_{\Gamma^{(1)*}} (p_i^{(1)}(\mathbf{y}, \tau) K_{ij}^{(1)}(\mathbf{x}, \mathbf{y}, t - \tau) - u_i^{(1)}(\mathbf{y}, \tau) F_{ij}^{(1)}(\mathbf{x}, \mathbf{y}, t - \tau)) d\mathbf{y} d\tau, \quad \mathbf{x} \in \Gamma^{(1)cr}, \quad (8)$$

$$\frac{1}{2} p_j^{(1)}(\mathbf{x}, t) = \int_T \int_{\Gamma^{(1)cr}} (g_i^{(1)}(\mathbf{y}, \tau) K_{ij}^{(1)}(\mathbf{x}, \mathbf{y}, t - \tau) - u_i^{(1)}(\mathbf{y}, \tau) F_{ij}^{(1)}(\mathbf{x}, \mathbf{y}, t - \tau)) d\mathbf{y} d\tau$$
$$+ \int_T \int_{\Gamma^{(1)*}} (p_i^{(1)}(\mathbf{y}, \tau) K_{ij}^{(1)}(\mathbf{x}, \mathbf{y}, t - \tau) - u_i^{(1)}(\mathbf{y}, \tau) F_{ij}^{(1)}(\mathbf{x}, \mathbf{y}, t - \tau)) d\mathbf{y} d\tau, \quad \mathbf{x} \in \Gamma^{(1)*}, \quad (9)$$

$$\frac{1}{2} g_j^{(2)}(\mathbf{x}, t) = \int_T \int_{\Gamma^{(2)cr}} (g_i^{(2)}(\mathbf{y}, \tau) K_{ij}^{(2)}(\mathbf{x}, \mathbf{y}, t - \tau) - u_i^{(2)}(\mathbf{y}, \tau) F_{ij}^{(2)}(\mathbf{x}, \mathbf{y}, t - \tau)) d\mathbf{y} d\tau$$
$$+ \int_T \int_{\Gamma^{(2)*}} (p_i^{(2)}(\mathbf{y}, \tau) K_{ij}^{(2)}(\mathbf{x}, \mathbf{y}, t - \tau) - u_i^{(2)}(\mathbf{y}, \tau) F_{ij}^{(2)}(\mathbf{x}, \mathbf{y}, t - \tau)) d\mathbf{y} d\tau, \quad \mathbf{x} \in \Gamma^{(2)cr}, \quad (10)$$

$$\frac{1}{2} p_j^{(2)}(\mathbf{x}, t) = \int_T \int_{\Gamma^{(2)cr}} (g_i^{(2)}(\mathbf{y}, \tau) K_{ij}^{(2)}(\mathbf{x}, \mathbf{y}, t - \tau) - u_i^{(2)}(\mathbf{y}, \tau) F_{ij}^{(2)}(\mathbf{x}, \mathbf{y}, t - \tau)) d\mathbf{y} d\tau$$
$$+ \int_T \int_{\Gamma^{(2)*}} (p_i^{(2)}(\mathbf{y}, \tau) K_{ij}^{(2)}(\mathbf{x}, \mathbf{y}, t - \tau) - u_i^{(2)}(\mathbf{y}, \tau) F_{ij}^{(2)}(\mathbf{x}, \mathbf{y}, t - \tau)) d\mathbf{y} d\tau, \quad \mathbf{x} \in \Gamma^{(2)*}. \quad (11)$$

Finally, the system of boundary integral equations takes the form:

$$\frac{1}{2} g_j^{(1)}(\mathbf{x}, t) - \int_T \int_{\Gamma^{(1)cr}} g_i^{(1)}(\mathbf{y}, \tau) K_{ij}^{(1)}(\mathbf{x}, \mathbf{y}, t - \tau) d\mathbf{y} d\tau = - \int_T \int_{\Gamma^{(1)cr}} u_i^{(1)}(\mathbf{y}, \tau) F_{ij}^{(1)}(\mathbf{x}, \mathbf{y}, t - \tau) d\mathbf{y} d\tau$$
$$+ \int_T \int_{\Gamma^*} (u_i^*(\mathbf{y}, \tau) F_{ij}^{(1)}(\mathbf{x}, \mathbf{y}, t - \tau) - p_i^*(\mathbf{y}, \tau) K_{ij}^{(1)}(\mathbf{x}, \mathbf{y}, t - \tau)) d\mathbf{y} d\tau, \quad \mathbf{x} \in \Gamma^{(1)cr}, \quad (12)$$

$$\frac{1}{2} g_j^{(2)}(\mathbf{x}, t) - \int_T \int_{\Gamma^{(2)cr}} g_i^{(2)}(\mathbf{y}, \tau) K_{ij}^{(2)}(\mathbf{x}, \mathbf{y}, t - \tau) d\mathbf{y} d\tau = - \int_T \int_{\Gamma^{(2)cr}} u_i^{(2)}(\mathbf{y}, \tau) F_{ij}^{(2)}(\mathbf{x}, \mathbf{y}, t - \tau) d\mathbf{y} d\tau$$
$$- \int_T \int_{\Gamma^*} (u_i^*(\mathbf{y}, \tau) F_{ij}^{(2)}(\mathbf{x}, \mathbf{y}, t - \tau) - p_i^*(\mathbf{y}, \tau) K_{ij}^{(2)}(\mathbf{x}, \mathbf{y}, t - \tau)) d\mathbf{y} d\tau, \quad \mathbf{x} \in \Gamma^{(2)cr}, \quad (13)$$

$$\int_T \int_{\Gamma^{(1)cr}} g_i^{(1)}(\mathbf{y}, \tau) K_{ij}^{(1)}(\mathbf{x}, \mathbf{y}, t - \tau) d\mathbf{y} d\tau = \frac{1}{2} p_j^*(\mathbf{x}, t) + \int_T \int_{\Gamma^{(1)cr}} u_i^{(1)}(\mathbf{y}, \tau) F_{ij}^{(1)}(\mathbf{x}, \mathbf{y}, t - \tau) d\mathbf{y} d\tau$$
$$- \int_T \int_{\Gamma^*} (u_i^*(\mathbf{y}, \tau) F_{ij}^{(1)}(\mathbf{x}, \mathbf{y}, t - \tau) - p_i^*(\mathbf{y}, \tau) K_{ij}^{(1)}(\mathbf{x}, \mathbf{y}, t - \tau)) d\mathbf{y} d\tau, \quad \mathbf{x} \in \Gamma^*, \quad (14)$$

$$\int_T \int_{\Gamma^{(2)cr}} g_i^{(2)}(\mathbf{y}, \tau) K_{ij}^{(2)}(\mathbf{x}, \mathbf{y}, t - \tau) d\mathbf{y} d\tau = \frac{1}{2} p_j^*(\mathbf{x}, t) + \int_T \int_{\Gamma^{(2)cr}} u_i^{(2)}(\mathbf{y}, \tau) F_{ij}^{(2)}(\mathbf{x}, \mathbf{y}, t - \tau) d\mathbf{y} d\tau$$
$$+ \int_T \int_{\Gamma^*} (u_i^*(\mathbf{y}, \tau) F_{ij}^{(2)}(\mathbf{x}, \mathbf{y}, t - \tau) - p_i^*(\mathbf{y}, \tau) K_{ij}^{(2)}(\mathbf{x}, \mathbf{y}, t - \tau)) d\mathbf{y} d\tau, \quad \mathbf{x} \in \Gamma^*. \quad (15)$$

When considering an interface, we integrated over the surface Γ^* with the outer normal vector $\mathbf{n}_{\Gamma^*} = \mathbf{n}_{\Gamma^{(2)*}} = -\mathbf{n}_{\Gamma^{(1)*}}$. This entailed the corresponding changes of the signs of integrals in Eqs. (10) and (11). We also introduced the following new variables according to the bonding conditions (2):

$$u_i^*(\mathbf{x}, t) = u_i^{(1)}(\mathbf{x}, t), \qquad p_i^*(\mathbf{x}, t) = -p_i^{(1)}(\mathbf{x}, t), \quad \mathbf{x} \in \Gamma^{(1)*}, \ t \in T,$$
$$u_i^*(\mathbf{x}, t) = u_i^{(2)}(\mathbf{x}, t), \qquad p_i^*(\mathbf{x}, t) = p_i^{(2)}(\mathbf{x}, t), \quad \mathbf{x} \in \Gamma^{(2)*}, \ t \in T.$$

For the case of harmonic loading with the frequency $\omega = 2\pi/T$, which is considered in the paper, all physical quantities are harmonic functions and can be presented as follows:

$$f(\bullet, t) = \text{Re}(f(\bullet)e^{i\omega t}), \qquad f(\bullet) = \frac{\omega}{2\pi} \int_0^T f(\bullet, t)e^{-i\omega t} dt.$$

Then the system of boundary integral equations (12)–(15) can be rewritten as:

$$\frac{1}{2} g_j^{(1)}(\mathbf{x}) - \int_{\Gamma^{(1)cr}} g_i^{(1)}(\mathbf{y}) K_{ij}^{(1)}(\mathbf{x}, \mathbf{y}, \omega) d\mathbf{y}$$
$$= -\int_{\Gamma^{(1)cr}} u_i^{(1)}(\mathbf{y}) F_{ij}^{(1)}(\mathbf{x}, \mathbf{y}, \omega) d\mathbf{y} + \int_{\Gamma^*} (u_i^*(\mathbf{y}) F_{ij}^{(1)}(\mathbf{x}, \mathbf{y}, \omega) - p_i^*(\mathbf{y}) K_{ij}^{(1)}(\mathbf{x}, \mathbf{y}, \omega)) d\mathbf{y}, \quad \mathbf{x} \in \Gamma^{(1)cr}, \tag{16}$$

$$\frac{1}{2} g_j^{(2)}(\mathbf{x}) - \int_{\Gamma^{(2)cr}} g_i^{(2)}(\mathbf{y}) K_{ij}^{(2)}(\mathbf{x}, \mathbf{y}, \omega) d\mathbf{y}$$
$$= -\int_{\Gamma^{(2)cr}} u_i^{(2)}(\mathbf{y}) F_{ij}^{(2)}(\mathbf{x}, \mathbf{y}, \omega) d\mathbf{y} - \int_{\Gamma^*} (u_i^*(\mathbf{y}) F_{ij}^{(2)}(\mathbf{x}, \mathbf{y}, \omega) - p_i^*(\mathbf{y}) K_{ij}^{(2)}(\mathbf{x}, \mathbf{y}, \omega)) d\mathbf{y}, \quad \mathbf{x} \in \Gamma^{(2)cr}, \tag{17}$$

$$\int_{\Gamma^{(1)cr}} g_i^{(1)}(\mathbf{y}) K_{ij}^{(1)}(\mathbf{x}, \mathbf{y}, \omega) d\mathbf{y} = \frac{1}{2} p_j^*(\mathbf{x}) + \int_{\Gamma^{(1)cr}} u_i^{(1)}(\mathbf{y}) F_{ij}^{(1)}(\mathbf{x}, \mathbf{y}, \omega) d\mathbf{y}$$
$$- \int_{\Gamma^*} (u_i^*(\mathbf{y}) F_{ij}^{(1)}(\mathbf{x}, \mathbf{y}, \omega) - p_i^*(\mathbf{y}) K_{ij}^{(1)}(\mathbf{x}, \mathbf{y}, \omega)) d\mathbf{y}, \quad \mathbf{x} \in \Gamma^*, \tag{18}$$

$$\int_{\Gamma^{(2)cr}} g_i^{(2)}(\mathbf{y}) K_{ij}^{(2)}(\mathbf{x}, \mathbf{y}, \omega) d\mathbf{y} = \frac{1}{2} p_j^*(\mathbf{x}) + \int_{\Gamma^{(2)cr}} u_i^{(2)}(\mathbf{y}) F_{ij}^{(2)}(\mathbf{x}, \mathbf{y}, \omega) d\mathbf{y}$$
$$+ \int_{\Gamma^*} (u_i^*(\mathbf{y}) F_{ij}^{(2)}(\mathbf{x}, \mathbf{y}, \omega) - p_i^*(\mathbf{y}) K_{ij}^{(2)}(\mathbf{x}, \mathbf{y}, \omega)) d\mathbf{y}, \quad \mathbf{x} \in \Gamma^*. \tag{19}$$

For the considered case of an interface linear crack under harmonic loading the Green fundamental displacement tensor has the following form [2,6]:

$$U_{12}^{(m)}(\mathbf{x}, \mathbf{y}, \omega) = U_{21}^{(m)}(\mathbf{x}, \mathbf{y}, \omega) = 0, \tag{20}$$

$$U_{11}^{(m)}(\mathbf{x}, \mathbf{y}, \omega) = \frac{i}{4\mu^{(m)}} \left[H_0^{(1)}\left(\frac{\omega r}{c_2^{(m)}}\right) + \frac{c_2^{(m)}}{\omega r} H_1^{(1)}\left(\frac{\omega r}{c_2^{(m)}}\right) - \frac{\left(c_2^{(m)}\right)^2}{c_1^{(m)} \omega r} H_1^{(1)}\left(\frac{\omega r}{c_1^{(m)}}\right) \right.$$
$$\left. - H_2^{(1)}\left(\frac{\omega r}{c_2^{(m)}}\right) + \frac{\mu^{(m)}}{\lambda^{(m)} + 2\mu^{(m)}} H_2^{(1)}\left(\frac{\omega r}{c_1^{(m)}}\right) \right], \tag{21}$$

$$U_{22}^{(m)}(\mathbf{x}, \mathbf{y}, \omega) = \frac{i}{4\mu^{(m)}} \left[H_0^{(1)}\left(\frac{\omega r}{c_2^{(m)}}\right) + \frac{c_2^{(m)}}{\omega r} H_1^{(1)}\left(\frac{\omega r}{c_2^{(m)}}\right) - \frac{\left(c_2^{(m)}\right)^2}{c_1^{(m)} \omega r} H_1^{(1)}\left(\frac{\omega r}{c_1^{(m)}}\right) \right], \tag{22}$$

where $H_n^{(1)}(\bullet)$ are the Hankel functions of the first kind [22]; $r = |x_1 - y_1|$ is the distance between the points $\mathbf{x}$ and $\mathbf{y}$; $c_1^{(m)} = \sqrt{(\lambda^{(m)} + 2\mu^{(m)})/\rho^{(m)}}$ and $c_2^{(m)} = \sqrt{\mu^{(m)}/\rho^{(m)}}$ are velocities of the longitudinal and transversal waves respectively.

The corresponding integral kernels $K_{ij}^{(m)}(\mathbf{x}, \mathbf{y}, \omega)$ and $F_{ij}^{(m)}(\mathbf{x}, \mathbf{y}, \omega)$ for the case when $\mathbf{n}(\mathbf{x}) = \mathbf{n}(\mathbf{y}) = (0, 1)$ are as follows:

$$K_{11}^{(m)}(\mathbf{x}, \mathbf{y}, \omega) = K_{22}^{(m)}(\mathbf{x}, \mathbf{y}, \omega) = 0, \tag{23}$$

$$K_{12}^{(m)}(\mathbf{x}, \mathbf{y}, \omega) = \frac{i}{4} \frac{\partial r}{\partial x_1} \left[\left(\frac{\omega}{c_2^{(m)}}\right) H_1^{(1)}\left(\frac{\omega r}{c_2^{(m)}}\right) - \frac{2}{r} H_2^{(1)}\left(\frac{\omega r}{c_2^{(m)}}\right) + \frac{2}{r} \frac{\mu^{(m)}}{\lambda^{(m)} + 2\mu^{(m)}} H_2^{(1)}\left(\frac{\omega r}{c_1^{(m)}}\right) \right], \tag{24}$$

$$K_{21}^{(m)}(\mathbf{x}, \mathbf{y}, \omega) = \frac{i}{4} \frac{\partial r}{\partial x_1} \left[\frac{\lambda^{(m)}}{\lambda^{(m)} + 2\mu^{(m)}} \left(\frac{\omega}{c_1^{(m)}} \right) H_1^{(1)} \left(\frac{\omega r}{c_1^{(m)}} \right) - \frac{1}{r} \frac{\lambda^{(m)} + 2\mu^{(m)}}{\mu^{(m)}} H_2^{(1)} \left(\frac{\omega r}{c_2^{(m)}} \right) + \frac{1}{r} H_2^{(1)} \left(\frac{\omega r}{c_1^{(m)}} \right) \right], \quad (25)$$

$$F_{12}^{(m)}(\mathbf{x}, \mathbf{y}, \omega) = F_{21}^{(m)}(\mathbf{x}, \mathbf{y}, \omega) = 0, \quad (26)$$

$$F_{11}^{(m)}(\mathbf{x}, \mathbf{y}, \omega) = \frac{i\mu^{(m)}}{4} \left[\left(\frac{\omega}{c_2^{(m)}} \right)^2 H_0^{(1)} \left(\frac{\omega r}{c_2^{(m)}} \right) - 4 \frac{\omega}{c_2^{(m)} r} H_1^{(1)} \left(\frac{\omega r}{c_2^{(m)}} \right) \right.$$

$$\left. + 4 \frac{\mu^{(m)}}{\lambda^{(m)} + 2\mu^{(m)}} \frac{\omega}{c_1^{(m)} r} H_1^{(1)} \left(\frac{\omega r}{c_1^{(m)}} \right) + \frac{12}{r^2} \left(H_2^{(1)} \left(\frac{\omega r}{c_2^{(m)}} \right) - \frac{\mu^{(m)}}{\lambda^{(m)} + 2\mu^{(m)}} H_2^{(1)} \left(\frac{\omega r}{c_1^{(m)}} \right) \right) \right], \quad (27)$$

$$F_{22}^{(m)}(\mathbf{x}, \mathbf{y}, \omega) = \frac{i\mu^{(m)}}{2} \left[\left(\frac{\lambda^{(m)}}{\lambda^{(m)} + 2\mu^{(m)}} \right)^2 \left(\frac{\omega}{c_2^{(m)}} \right)^2 H_0^{(1)} \left(\frac{\omega r}{c_1^{(m)}} \right) + 2 \frac{\omega}{c_2^{(m)} r} H_1^{(1)} \left(\frac{\omega r}{c_2^{(m)}} \right) \right.$$

$$\left. + 2 \frac{\omega}{c_1^{(m)} r} \frac{\lambda^{(m)}}{\lambda^{(m)} + 2\mu^{(m)}} H_1^{(1)} \left(\frac{\omega r}{c_1^{(m)}} \right) - \frac{6}{r^2} \left(H_2^{(1)} \left(\frac{\omega r}{c_2^{(m)}} \right) - \frac{\mu^{(m)}}{\lambda^{(m)} + 2\mu^{(m)}} H_2^{(1)} \left(\frac{\omega r}{c_1^{(m)}} \right) \right) \right]. \quad (28)$$

Note that in the present study the form of the resulting systems of boundary integral equations (12)–(15) and (16)–(19) differs significantly from the corresponding systems in [14–16,18]. Eqs. (14) and (15) were obtained directly from Eqs. (9) and (11) without using representations for the displacements at the interface. Therefore the resulting system of boundary integral equations becomes simpler, it does not contain integral kernels $U_{ij}^{(m)}(\mathbf{x}, \mathbf{y}, t - \tau)$ and $W_{ij}^{(m)}(\mathbf{x}, \mathbf{y}, t - \tau)$. The further algebraic manipulations (i.e. summation and subtraction of the corresponding integral equations) are also unnecessary, therefore the system of boundary integral equations does not contain residuals of all integral kernels and the corresponding matrix of linear algebraic equations becomes sparser. In particular, for the case of the collocation method with a piecewise continuous approximation used in the current paper, the number of non-zero elements of the matrix of linear algebraic equations decreases by $8N_{\text{out}}(N_{\text{in}} - 1)$, where N_{out} and N_{in} are the numbers of boundary elements located on the bonding interface and crack surface respectively. Consequently the total number of integrals over boundary elements, required to be computed in order to solve the problem, decreases even further, by $4N_{\text{out}}(4N_{\text{in}} + 4N_{\text{out}})$, which results in the significant acceleration of the numerical solution of the problem. On average, the solution time decreases by 40%–50%. The stability of the obtained solution also increases, especially for the higher frequencies of external loading and for the cases with considerable difference between mechanical properties of adjoining half-spaces.

It is worth mentioning that due to the presence of non-integrable singularities in the integral kernels $F_{ij}^{(m)}(\mathbf{x}, \mathbf{y}, \omega)$, whose rank exceeds the dimension of the integration region, the corresponding hypersingular integrals of the system of boundary integral equations (16)–(19) are treated in the sense of the Hadamard finite part [6,23,24].

4. Numerical results

As a numerical example let us consider an incident time-harmonic tension–compression wave of the unit intensity propagating in the normal direction to the interface of the linear crack with length of $2R$. Poisson's ratios for the materials are specified as $\nu^{(1)} = 0.3$ and $\nu^{(2)} = 0.25$, and the ratios of their Young's moduli and material densities are specified as $E^{(1)}/E^{(2)} = 2.0$ and $\rho^{(1)}/\rho^{(2)} = 3.0$, respectively.

The piecewise constant approximation of the known and unknown functions was used to solve the problem numerically. The normal and tangential displacements at the bonding interface are given in Fig. 2 for the reduced wave number $k_2^{(1)}R = 0.05$, where $k_2^{(1)} = \omega/c_2^{(1)}$, $c_2^{(1)}$ is the velocity of the transversal wave in the upper half-space. The maximal in time normal and tangential displacement discontinuities at the crack surface are given in Fig. 3 for different values of the reduced wave number $k_2^{(1)}R$. Results are normalized by the factor $2\mu_0/Rp_0$, where p_0 is the stress amplitude of the incident wave and μ_0 is specified as follows [11]:

$$\mu_0 = \mu^{(1)} \frac{1 - \gamma_2}{1 + \kappa^{(1)}}, \quad \gamma_2 = \left(\frac{a_1}{2} - a_2 \right), \quad a_1 = \frac{\mu^{(1)} - \mu^{(2)}}{\mu^{(1)} + \kappa^{(1)}\mu^{(2)}}, a_2 = \frac{\kappa^{(1)}\mu^{(2)} - \kappa^{(2)}\mu^{(1)}}{2(\mu^{(2)} + \kappa^{(2)}\mu^{(1)})}, \kappa^{(m)} = 3 - 4\nu^{(m)}. \quad (29)$$

Note that the solution is symmetric with respect to the centre of the crack and the Sommerfeld radiation-type condition (3) is satisfied at the infinity, i.e. the displacements at the bonding interface decrease gradually with increase in the distance to the crack.

In order to validate the method proposed, the obtained solution was compared with the numerical static solution [11]. When the frequency tends to zero, the solution of the dynamic problem tends to the solution of the corresponding static problem. In Fig. 4 the maximal displacements of the opposite crack faces and displacement discontinuities are given for the case of a small wave number $k_2^{(1)}R = 0.01$. Poisson's ratios for the materials are $\nu^{(1)} = 0.35$ and $\nu^{(2)} = 0.3$, and the ratio of
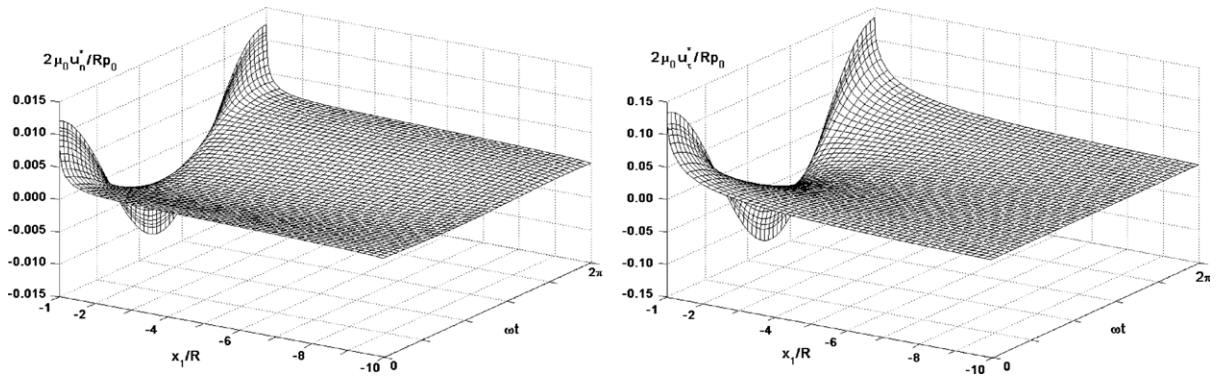
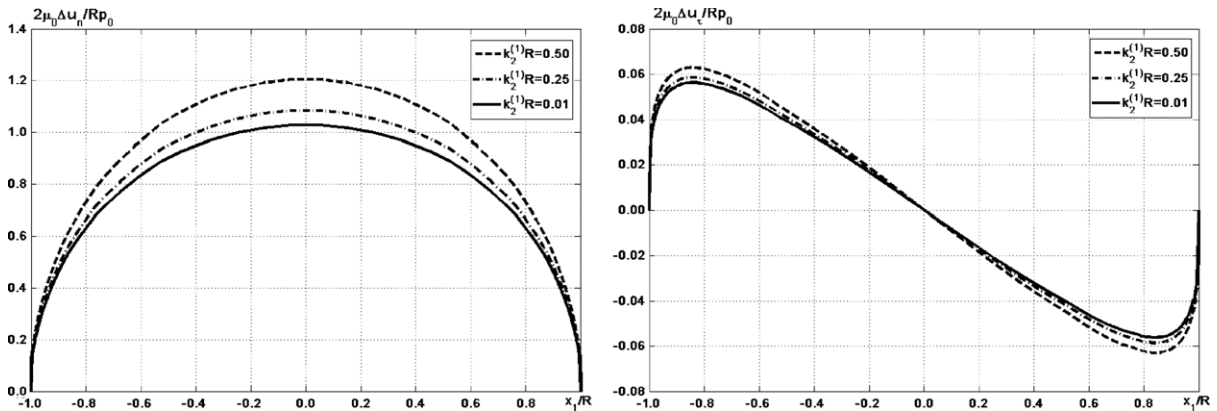**Fig. 2.** Normal and tangential displacements at the bonding interface.

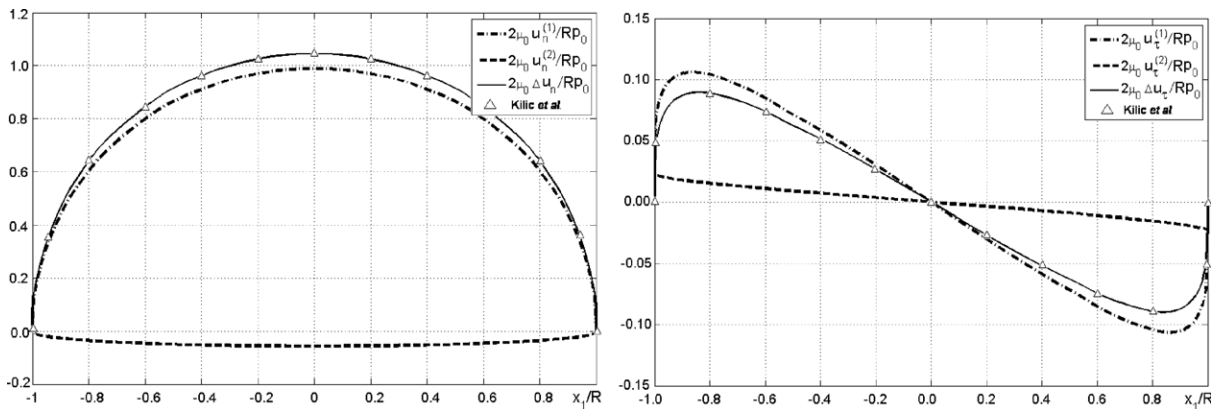**Fig. 3.** Maximal displacement discontinuities at the crack surface.

Fig. 4. Maximal displacements and displacement discontinuities at the crack surface.

shear moduli is $\mu^{(2)}/\mu^{(1)} = 20$. Note that the obtained numerical results are in a very good agreement with those presented in [11].

5. Future work

In reality, under dynamic loading the opposite crack faces interact with each other, significantly changing the stress and strain fields near the crack tips. However, since the area of interest is hidden in the solid, the direct observation and measurement of the contact characteristics is impossible. The nature of the contact interaction between two opposite crack surfaces is very complex. Under deformation of the material, the contact area changes in time and it is unknown beforehand and must be determined as a part of solution. The complexity of the problem is further compounded by the fact that

the contact behaviour is very sensitive to the material properties of two contacting surface, their textures and topologies, frequency, magnitude and direction of the external loading in relation to the contact region [25,26,24]. Taking these effects into account will make the contact crack problem highly non-linear. Thus considering the crack closure effect is the natural next stage of this research.

Under the external dynamic loading the opposite crack faces move with respect to each other and the corresponding displacement is given by the discontinuity vector $\Delta\mathbf{u}(\mathbf{x}, t) = \mathbf{u}^{(1)}(\mathbf{x}, t) - \mathbf{u}^{(2)}(\mathbf{x}, t)$. The contact interaction results in the appearance of the contact force $\mathbf{q}(\mathbf{x}, t)$ in the contact region.

In order to include contact interaction into consideration, the Signorini constraints must be imposed for the normal components of the contact force and the displacement discontinuity vectors on the middle surface of the crack, Ω:

$$\Delta u_n(\mathbf{x}, t) \geq 0, \qquad q_n(\mathbf{x}, t) \geq 0, \qquad \Delta u_n(\mathbf{x}, t) q_n(\mathbf{x}, t) = 0, \quad \mathbf{x} \in \Omega, t \in [0; T]. \tag{30}$$

The constraints ensure that there is no interpenetration of the opposite crack faces (the first constraint in Eq. (30)); the contact force is unilateral (the second constraint in Eq. (30)); and the contact forces are absent if there is a non-zero opening of the crack (the third constraint in Eq. (30)).

Additionally we assume that the contact interaction satisfies the Coulomb friction law:

$$|q_\tau(\mathbf{x}, t)| < k_\tau q_n(\mathbf{x}, t) \Rightarrow \frac{\partial \Delta u_\tau(\mathbf{x}, t)}{\partial t} = 0; \tag{31}$$

$$|q_\tau(\mathbf{x}, t)| = k_\tau q_n(\mathbf{x}, t) \Rightarrow \frac{\partial \Delta u_\tau(\mathbf{x}, t)}{\partial t} = -\frac{q_\tau(\mathbf{x}, t)}{|q_\tau(\mathbf{x}, t)|} \left| \frac{\partial \Delta u_\tau(\mathbf{x}, t)}{\partial t} \right|, \quad \mathbf{x} \in \Omega, t \in [0; T], \tag{32}$$

where k_τ is the friction coefficient. Eq. (31) means that the opposite crack faces remain immovable with respect to each other in the tangential plane as long as they are held by the friction force. However, as soon as the magnitude of the tangential contact forces reaches a certain limit, depending on the friction coefficient and the normal contact forces (see Eq. (32)), the crack faces begin to slip.

If the contact interaction of crack faces is taken into account, the resulting process is a steady-state periodic process, but not a harmonic one. As a result, components of the stress–strain state cannot be represented as a function of coordinates multiplied by an exponential function. According to [6,7,24], all components of solution can be expanded into the Fourier series

$$f(\bullet, t) = \frac{f_{0,\cos}(\bullet)}{2} + \sum_{k=1}^{\infty} (f_{k,\cos}(\bullet) \cos(\omega_k t) + f_{k,\sin}(\bullet) \sin(\omega_k t)), \tag{33}$$

where $\omega_k = 2\pi k/T$, and Fourier coefficients are given as

$$f_{k,\cos}(\bullet) = \frac{\omega}{2\pi} \int_0^T f(\bullet, t) \cos(\omega_k t) \mathrm{d}t, \qquad f_{k,\sin}(\bullet) = \frac{\omega}{2\pi} \int_0^T f(\bullet, t) \sin(\omega_k t) \mathrm{d}t. \tag{34}$$

The considered contact problem is non-linear and requires an iterative solution procedure. During the iterative process, the Fourier coefficients will change from one iterative step to the next until the distribution of the displacements and contact force vectors satisfying the constraints (30)–(32) will be found.

6. Conclusions

The problem for an interface linear crack between dissimilar elastic materials under harmonic loading was solved by the boundary integral equations method. For the numerical solution the collocation method with piecewise constant approximation on each boundary element was used. The distributions of the displacements and traction at the bimaterial interface were computed for different values of the frequency of the incident tension–compression wave. The obtained dynamic solution was compared with the corresponding static solution.

Acknowledgements

References

[1] M.H. Aliabadi, D.P. Rook, Numerical Fracture Mechanics, Computational Mechanics Publications and Kluwer Academic Publishers, 1991.
[2] S. Balas, J. Sladek, V. Sladek, Stress Analysis by Boundary Element Methods, Elsevier, 1989.
[3] T.A. Cruse, Boundary Element Analysis in Computational Fracture Mechanics, Kluwer Academic Publisher, 1988.
[4] J. Dominguez, R. Gallego, Fundamentals of dynamic and BEM for dynamic fracture mechanics, in: M.H. Aliabadi, C.A. Brebbia, V.Z. Parton (Eds.), Static and Dynamic Fracture Mechanics, Computational Mechanics Publications, Southampton, 1994.
[5] K.F. Graff, Wave Motion in Elastic Solids, Dover Publications, 1991.

[6] A.N. Guz, V.V. Zozulya, Elastodynamic unilateral contact problems with friction for bodies with cracks, Internat. Appl. Mech. 38 (8) (2002) 895–932.

[7] A.N. Guz, V.V. Zozulya, Fracture dynamics with allowance for a crack edges contact interaction, Int. J. Nonlinear Sci. Numer. Simul. 2 (3) (2001) 173–233.

[8] Ch. Zhang, D. Gross, On Wave Propagation in Elastic Solids with Cracks, Computational Mechanics Publications, 1998.

[9] M. Comninou, The interface crack, J. Appl. Mech. 44 (1977) 631–636.

[10] L. Gorbatikh, Mathematical and computational aspects of nonuniform frictional slip modelling, J. Comput. Appl. Math. 168 (1–2) (2004) 215–224.

[11] B. Kilic, E. Madenci, R. Mahajan, Energy release rate and contact zone in a cohesive and an interface crack by hypersingular integral equations, Internat. J. Solids Structures 43 (2006) 1159–1188.

[12] V. Mantic, A. Blazquez, E. Correa, F. Paris, Analysis of interface cracks with contact in composites by 2D BEM, in: M. Guagliano, M.H. Aliabadi (Eds.), Fracture and Damage of Composites, WIT Press, 2006.

[13] J.R. Rice, Elastic fracture mechanics concepts for interfacial cracks, J. Appl. Mech. 55 (1) (1988) 98–103.

[14] I.A. Guz, O.V. Menshykov, V.A. Menshykov, Application of boundary integral equations to elastodynamics of an interface crack, Int. J. Fract. 140 (1–4) (2006) 277–284.

[15] O.V. Menshykov, I.A. Guz, V.A. Menshykov, Boundary integral equations in elastodynamics of interface crack, Philos. Trans. R. Soc. A 366 (2008) 1835–1839.

[16] O.V. Menshykov, V.A. Menshykov, I.A. Guz, The effect of frequency in the problem of interface crack under harmonic loading, Int. J. Fract. 146 (3) (2007) 197–202.

[17] O.V. Menshykov, V.A. Menshykov, I.A. Guz, Elastodynamics of a crack on the bimaterial interface, Eng. Anal. Bound. Elem. 33 (3) (2009) 294–301.

[18] V.A. Men'shikov, A.V. Men'shikov, I.A. Guz, Interfacial crack between elastic half-spaces under harmonic loading, Internat. Appl. Mech. 43 (8) (2007) 865–873.

[19] V.A. Men'shikov, A.V. Men'shikov, I.A. Guz, Passages to the limit in the dynamic problem for a crack at the interface between elastic media, Internat. Appl. Mech. 44 (7) (2008) 739–746.

[20] R.W. Goldstein, V.M. Vainshelbaum, Axisymmetric problem of a crack at the interface of layers in a multi-layered medium, Int. J. Eng. Sci. 14 (4) (1976) 335–352.

[21] V.I. Mossakovskii, M.T. Rybka, Generalization of the Griffith–Sneddon criterion for the case of a nonhomogeneous body, J. Appl. Math. Mech. 28 (6) (1964) 1277–1286.

[22] M. Abramowitz, I.A. Stegun, Handbook of Mathematical Functions with Formulas, Graphs, and Mathematical Tables, Dover Publications, 1964.

[23] P.A. Martin, F.J. Rizzo, I.R. Gonzalves, On hypersingular boundary integral equations for certain problems in mechanics, Mech. Res. Commun. 16 (1989) 65–71.

[24] O.V. Menshykov, M.V. Menshykova, I.A. Guz, Effect of friction of the crack faces for a linear crack under an oblique harmonic loading, Int. J. Eng. Sci. 46 (5) (2008) 438–458.

[25] O.V. Menshykov, I.A. Guz, Contact interaction of crack faces under oblique incidence of a harmonic wave, Int. J. Fract. 139 (1) (2006) 145–152.

[26] O.V. Menshykov, I.A. Guz, Effect of contact interaction of the crack faces for a crack under harmonic loading, Internat. Appl. Mech. 43 (7) (2007) 809–815.